Realization of a 4kW thermochemical segmented reactor in household scale for seasonal heat storage

Available online at www.sciencedirect.com

ScienceDirect

Energy Procedia 135 (2017) 105–114

Energy Procedia

www.elsevier.com/locate/procedia

11th International Renewable Energy Storage Conference, IRES 2017, 14-16 March 2017, Düsseldorf, Germany

Realization of a 4kW thermochemical segmented reactor in household scale for seasonal heat storage

M. Gaeini[a], M.R. Javed[a], H. Ouwerkerk[a], H.A. Zondag[a,b], C.C.M. Rindt[a,*]

[a]*Eindhoven University of Technology, Department of Mechanical Engineering, P.O.Box 513, 5600MB Eindhoven, The Netherlands*
[b]*ECN, Energy Research Center of the Netherlands, P.O. Box 1, 1755ZG Petten, The Netherlands*

Abstract

Replacing fossil fuel by solar energy as a promising sustainable energy source, is of high interest, for both electricity and heat generation. However, to reach high thermal solar fractions and to overcome the mismatch between supply and demand of solar heat, long term heat storage is necessary. A promising method for long term heat storage is to use thermochemical materials, TCMs. The reversible adsorption-desorption reactions, which are exothermic in the hydration direction and endothermic in the reverse dehydration direction, can be used to store heat. A 250L setup based on a gas-solid reaction between water-zeolite 13X is designed and tested. Humid air is introduced to a packed bed reactor filled with dehydrated material and by the resulting adsorption of water vapour on TCM, heat is released. The reactor consists of four segments of 62.5L each, which can be operated in different modes. The temperature is measured at several locations to gain insight into the effect of segmentation. Experiments are performed for hydration-dehydration cycles in different modes. Using the temperatures measured at different locations in the system, a complete thermal picture of the system is calculated, including thermal powers of the segments. A maximum power of around 4kW is obtained by running the segments in parallel mode. Compactness and robustness are two important factors for the successful introduction of heat storage systems in the built environment, and both can be met by reactor segmentation. With the segmented reactor concept, a high flexibility can be achieved in the performance of a heat storage system, while still being compact.

Peer-review under the responsibility of EUROSOLAR - The European Association for Renewable Energy.

Keywords:
Thermochemical heat storage; Open sorption system; Water-Zeolite; 250 L Pilot; Segmented packed bed reactor

1. Introduction

In Europe, energy consumption for domestic purposes accounts for almost 40 % of the total energy demand [1]. Therefore, in this sector, a significant potential exists to reduce fossil fuel consumption. Energy storage is a key step to shift to renewable energy sources, which are inherently intermittent. Solar energy, as one of the most exploitable renewable energy sources, is available more than required in residential houses during summer, while the demand

* Corresponding author.
E-mail address: C.C.M.Rindt@tue.nl

1876-6102
Peer-review under the responsibility of EUROSOLAR - The European Association for Renewable Energy.
10.1016/j.egypro.2017.09.491

cannot be met during winter. A solution is to store excess of solar energy in summer using a so-called thermal battery, which can be discharged to provide heat for the residential demand in winter [2].

A promising method is heat storage in thermochemical materials (TCM), by which heat can be stored in a compact and quasi loss-free way over a long time. In the thermochemical heat storage process, heat is stored into an endothermal dissociation reaction (charging), and, at a later time, the energy can be retrieved from the reverse exothermal reaction (discharging), according to the reaction $A(s) + B(g) \leftrightarrow AB(s) + heat$. Heat generated by a solar collector during summer can be employed to desorb water from the material. The energy stored in this way can be released during winter by introducing water vapor to the dehydrated material.

An interesting material should be non-toxic, non-corrosive and stable with fast reaction kinetics and high energy storage density [3]. A good candidate fulfilling these requirements is zeolite. Although zeolite is expensive to be used in a full scale seasonal heat storage, it is still a good candidate to be used in scientific studies because of its stability. In recent years, intense research has been performed on innovative system designs to integrate the thermochemical concept into an overall system, and lab or pilot scale setups are developed and tested. Table 1 presents some of the zeolite based prototypes that have been reported, along with operating conditions and energy densities.

Table 1: Prototypes along with operating conditions for open and closed systems.

project	material	charge temp. $[^oC]$	discharge temp. $[^oC]$	energy density $[kWh/m^3]$	max. power $[kW]$
MONOSORP [4]	70 kg zeolite 4A	170	20	120	1.5
STAID [5]	80 kg zeolite 13X	180	20	114	2.25
E-HUB/ECN [6]	150 kg zeolite 13X	185	25-60	58	0.4

The *MONOSORP* [4] prototype is developed based on zeolite honeycomb structures called monoliths instead of the ordinarily employed packed beds. The monoliths are made by extrusion of zeolite 4A into integrated shaped bodies with a large number of small straight channels inside. The main advantage of using such a material bed is low pressure drop. However, the monolith production adds up to the material cost. With an inlet temperature of about 20^oC and a humidity of $6g/kg$ (gram of water to kilogram of air) a maximum temperature lift of around 22^oC is achieved.

The *STAID* [5] prototype is a system consisting of two reactor segments, where zeolite 13X spherical particles are packed. The system can provide a maximum thermal power output of around $2.25kW$ during $6h$, with a maximum instantaneous COP (considering only electrical consumption during the hydration process) of 6.8. The inflow air has a relative humidity of around 70% at 20^oC, which corresponds to a water vapor pressure of about $16mbar$ or an absolute humidity of about $10g/kg$. This high value for the inlet humidity is the reason for the achieved high power.

The *E-HUB/ECN* [6] prototype is a system consisting of two packed bed reactor segments working with zeolite 13X. This system is developed such that it can provide thermal power at higher temperature compared to the above-mentioned systems. In this setup, an air-to-air heat exchanger is employed in order to preheat the inflow air by the residual heat in the outflow air. An inlet humidity of $12mbar$ water vapor pressure is applied. Air leakages inside the system lead to a low thermal power output from the system.

In this work, the implementation of thermochemical heat storage in the built environment utilizing solar thermal heat is investigated. Therefore, the operating conditions are chosen based on the application. Specifically, the inflow air should be conditioned carefully regarding the humidity, because the inflow humidity has a large effect on the output of the system. The segmentation concept is used in order to reduce heat losses. A large scale high power pilot is realized, consisting of four segments. Each reactor segment contains a $62.5L$ packed beds of the zeolite 13XBF material. The packed bed reactor design is chosen because of its simplicity and low cost, while the pressure drop over the bed is reduced by reducing the height-to-width ratio of the bed. The reactor segments are placed in a system with other components. Air leakage and high pressure are tried to be avoided in different parts of the system. Experiments are performed on the pilot in order to determine the energy storage density, demonstrate the power and calculate the COP. Recommendations are given for further studies on the pilot and for improvements.

2. Thermochemical heat storage in the built environment

Before a heat storage strategy is devised it is important to present an overview of the system being developed. Figure 1 shows the system overview for the charging and discharging processes. During the charging process in summer, air is blown through a heat exchanger to heat up to the desired temperature by the solar collector. During the discharge process in winter, humidified air from a borehole (i.e. $1300Pa$ water vapor pressure at 10^oC) gets preheated in an air-to-air heat exchanger by the outflow of the reactor and then passes through the reactor.

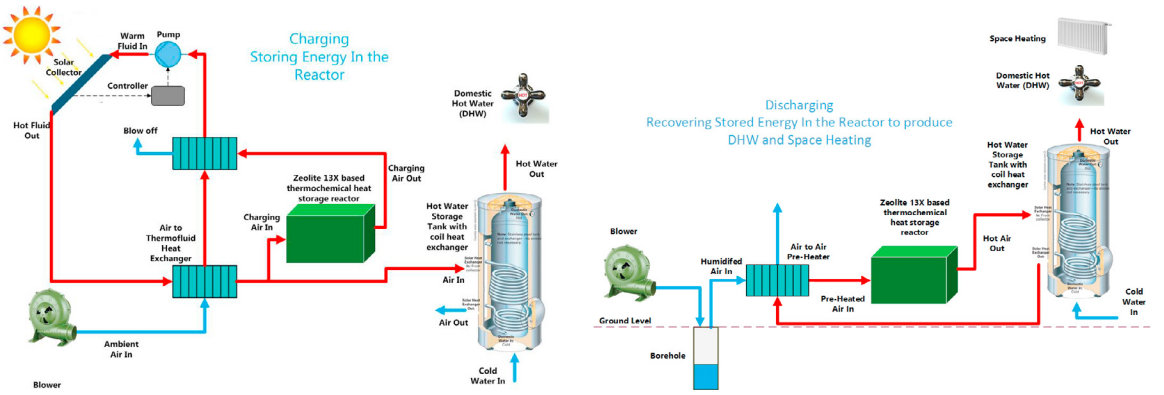

(a) charging process (b) discharging process

Fig. 1: Implementation of thermochemical heat storage system in residential building

As a reference for energy demand in buildings, the passive house standard is considered. For passive houses, the peak daily average heating and cooling loads are typically below $10W/m^2$ and annual useful energy demands are below $15kWh/m^2$ [7]. Considering a passive house with a floor area of $100m^2$, the total heat demand would be $1500kWh/year$ (which is in relatively low for average houses), and assuming an energy density of $180kWh/m^3$ for storage material, more than $8m^3$ of material is required to store the complete heat demand of the household.

If all the material is packed in a single reactor, the large thermal mass of the entire bed has to be heated up at once, which makes the performance of such a system (with all material packed in one reactor) slow, less controllable, and heat losses become large. Therefore, it is important to keep the reaction zone (the part of the material which participates in and/or is affected by the reaction) as small as possible. A method to reduce the reaction zone, which is denoted here as the segmentation concept, is to pack the material in separate reactor segments and to run only one segment at a time. The segmentation concept provides the simplicity and the low auxiliary energy need of the packed bed reactor design, and meets the limited reaction zone requirement. In this way, it is possible to run the segments in sequence with a constant power, while providing the required average demand. The produced energy can be stored in a short-term heat storage water tank, and the peak demand can be shaved by the water tank.

A monthly strategy can be developed, based on available solar energy, to calculate the number of segments that can be charged per day in a particular month. In addition, different strategies can be used in order to recover heat from one segment to another. By choosing a segment size of about $10kWh$, 200 segments would be needed to cover the complete annual heat demand of the house. However, the segment size needs to be optimized based on charging/discharging strategies.

The strategy which is chosen here for discharging is based on the average daily demand. In this way the thermochemical storage system operates continuously and the produced heat is stored in a short term storage tank. The short term hot water storage tank should be large enough to be able to cover the peak demand, while it is continuously charged by the thermochemical storage system. Considering a passive house with an average daily demand of $24kWh/day$, the required average power from the thermochemical reactor would be $1kW$. Assuming a temperature step of 20^oC in the reactor (based on experiments in a small scale setup [8]), an air flow rate of $50g/s$ is calculated for discharging the reactor.

3. Realization

At the Eindhoven University of Technology, a pilot setup is realized consisting of four segments. The pilot is designed to be able to provide $1kW$ thermal output per segment and $4kW$ combined, lasting for at least 10 hours. In this section, the realization of the pilot is explained at material, reactor and system level.

3.1. Material

The material zeolite 13XBF (CWK Chemiewerk Bad Köstritz GmbH) is used as thermochemical material consisting of spherical beads with an average diameter of $3.5mm$. An extensive discussion on the performance of the material is presented in previous work [8]. In each segment, $62.5L$ ($42.5kg$) of material is packed, with the possibility to increase it to $83.3L$ by adding more material in the top layer of the reactor.

3.2. Reactor

For the reactor segments a square prism (cuboid) shape is chosen, because of practical considerations in the realization of the pilot, as well as of a real system. Building the segments is practically much easier and cheaper with this shape. In addition, in a real system, segments can be stacked besides each other in a more compact way. In [9], an optimum diameter-to-height ratio of 1.5 is found for a cylindrical reactor. However, for a reactor with square cross-section, this ratio might be different. In this pilot, the aspect ratio is 2:1 (Width : Height). A detailed view of the designed reactor segment is shown in Figure 2. Two empty spaces, one at the top and one at the bottom of the material bed are embedded in each segment, as headers to ensure a uniform pressure drop over the bed, and hence, a uniform flow through the bed. The volume of each reactor segment (including empty spaces) is $114.75L$.

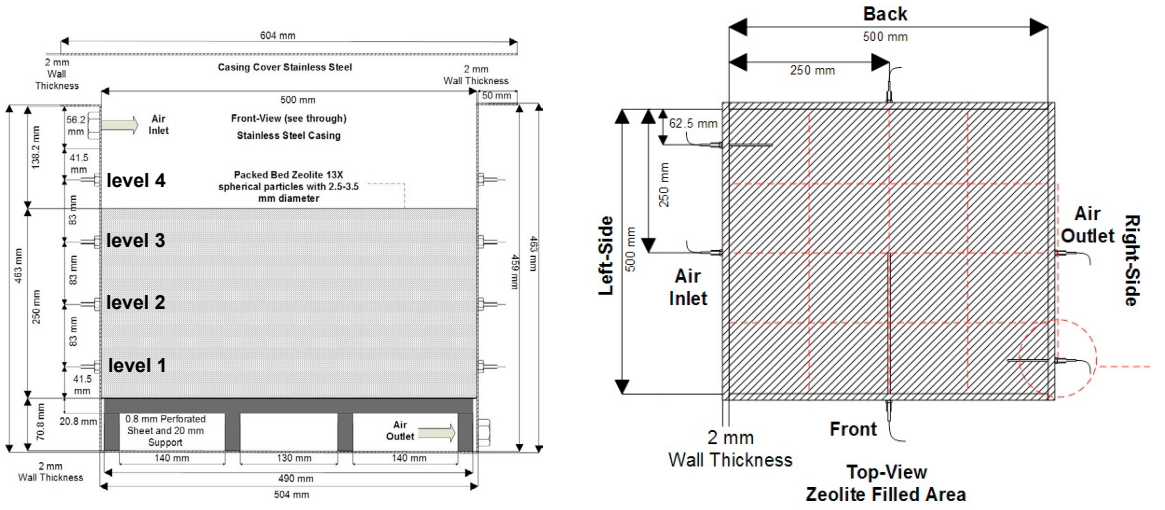

(a) side view (b) top view

Fig. 2: Detailed view of reactor

A stainless steel rectangular casing is realized as shown in Figure 3. The casing has a stainless steel cover which is bolted on the top side, and is made air tight with a sealant. The air inlet and outlet connections are on the top left and bottom right of the casing, respectively. The wall thickness of the casing is $2mm$, which forms a good balance between high mechanical strength and low thermal mass. A perforated sheet is used to hold the material bed in place at a certain height inside the reactor. The sheet is spot welded on top of a support structure placed at the bottom of the segment, in a way that the outlet is placed below the perforated sheet and the support. Another perforated sheet is used on top of the material to help the air distribution. An insulation layer made of glass wool with a thickness of $50mm$ is used on all sides of the casings.

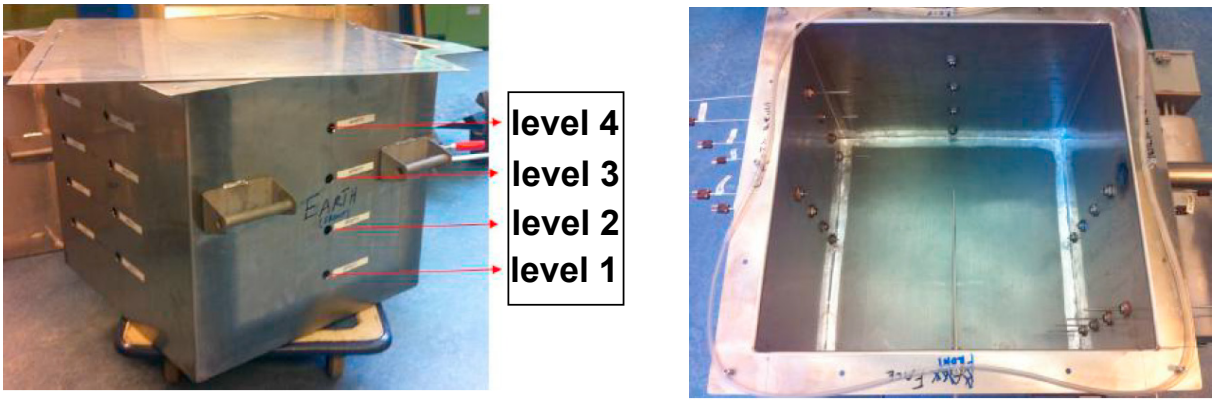

(a) side view (b) top view

Fig. 3: Pictures of realized reactor

As can be seen in Figure 2, each segment consists of four height levels which can be filled with material. However, in the present configuration that is used in this study, material is filed in the first three levels only (62.5L of material). In future studies, the material can be also filled up to the fourth level, which leads to having 83.3L of material in each segment. Inside one of the segments (denoted as segment 1), thermocouples are placed in order to analyze the internal behavior of the packed bed. The location of the thermocouples is chosen in a way that the effect of the flow distribution in the bed can be analyzed. By placing thermocouples in the corners of the packed bed, formation of any non-reactive zones inside the bed can be identified. The thermocouples are positioned at four different heights inside the reactor, and at each height there are six thermocouples.

3.3. System

A system is developed to accommodate the four reactor segments in the setup simulating the real thermochemical heat storage system for household application. A schematic view of the complete system is shown in Figure 4. In order to have flexibility in the operation of multiple segments, each segment is connected to an individual pipeline. Air flows into the system from the main inlet pipe, and then is divided over four paths. In each path, the air flow can be conditioned for either charging (dehydration) or discharging (hydration). The pressure and temperature of the flow are measured in the main pipe.

In each path, the flow rate is controlled and measured by a Mass Flow Controller capable of handling $50g/s$ flow with an accuracy of ±0.4%. A 3-way valve is used in order to direct the flow to the humidifier for the hydration process or bypass it for the dehydration process. During the hydration process the flow is humidified in a bubble column. The humidity of the flow is measured after the humidifier by a humidity-temperature sensor with a humidity accuracy of ±1.25% RH at 23^oC and temperature accuracy of $\pm 0.2^oC$. After the humidifier, another 3-way valve is used in order to blow off the flow during the stabilization time required for the humidifier. The temperature of the flow is measured after the valve by a Type T thermocouple with Stainless steel protective jacket with a thickness of $3.0mm$. The flow passes through a moisture-resistant heater with $7.7kW$ power and 300^oC maximum temperature, in order to heat up the dry air during the dehydration process or to preheat the humid air during the hydration process. After the heater, the pressure of the flow is measured by a pressure sensor with an accuracy of ±0.5%. Temperature is also measured at the inlet and outlet of the reactor with the same T-type of thermocouple as mentioned before. At the outlet, the humidity is measured by the same type of humidity sensor as at the inlet. The outlet of each reactor segment is connected to a check valve and then to the exhaust vent. The purpose of these check valves is to close the outlet when there is no flow after the experiments, to prevent any moisture being exchanged between the surroundings and the reactor segments via the outlet. A picture of the realized setup is shown in Figure 5.

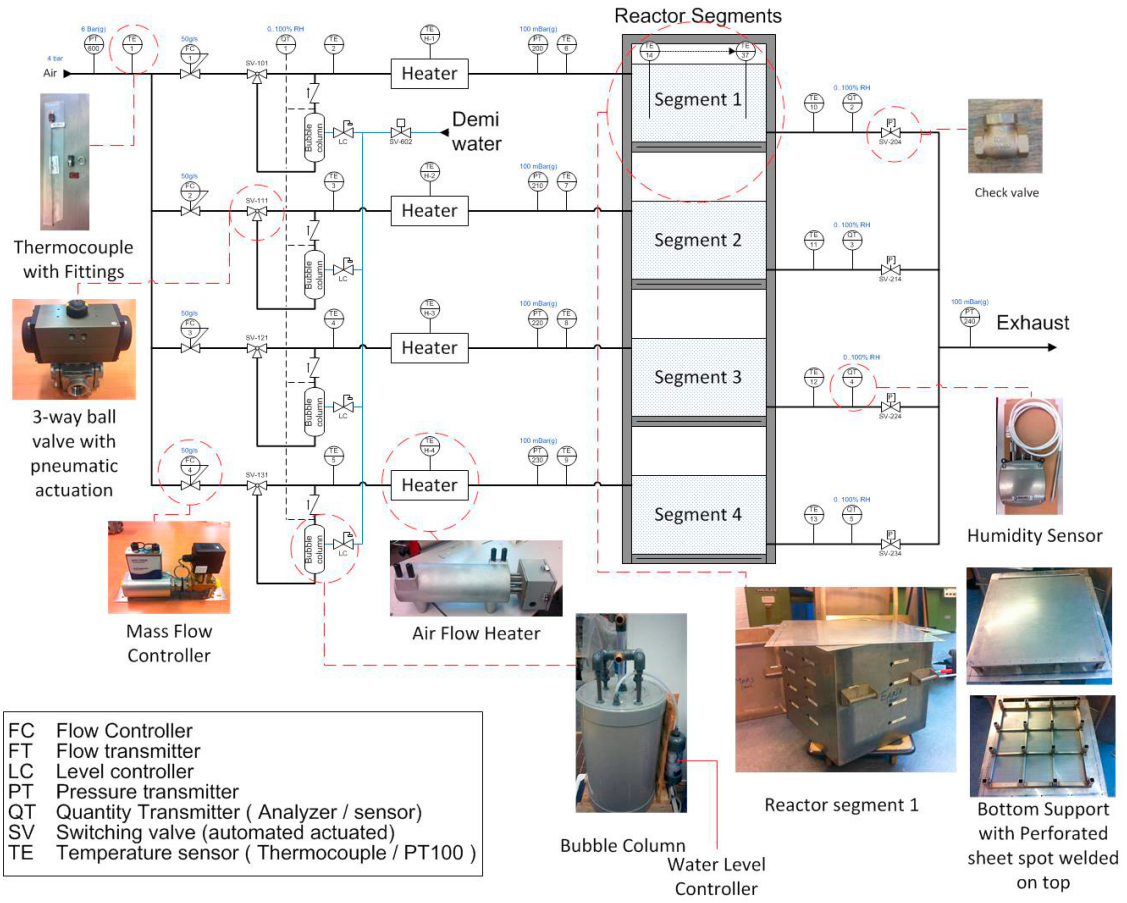

Fig. 4: Schematic view of system.

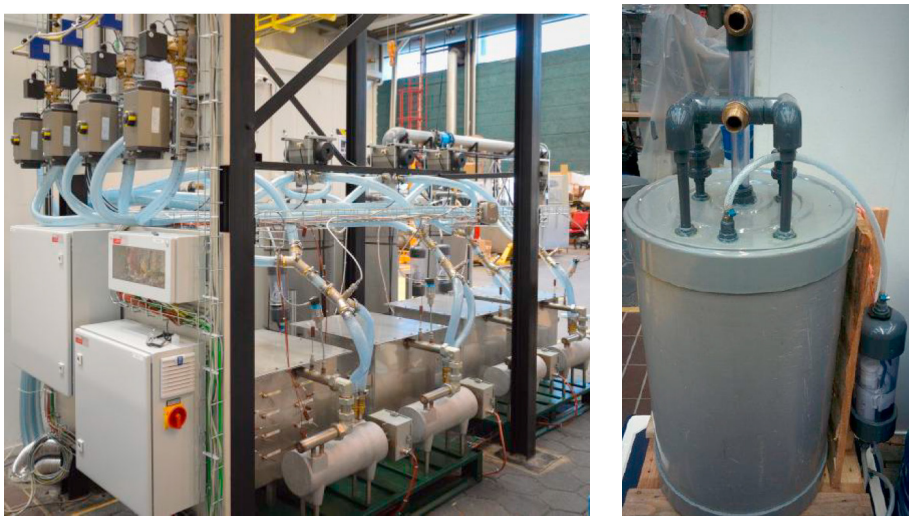

(a) complete system (b) humidifier

Fig. 5: Picture of realized system.

4. Experiments

The experiments are carried out with the pilot setup for de/re-hydration of the material beds in the segments. The experimental results of one dehydration (charging mode) and one rehydration (discharging mode) are discussed in this section. The experimental conditions for these two experiments are presented in Table 2.

Table 2: Operational conditions for the de/re-hydration experiments (values are for each segment).

parameter	unit	dehydration	rehydration
air flow rate	$[g/s]$	33	50
heater temperature	$[^oC]$	190	off
duration	$[h]$	7	18

The temperatures inside the bed and at the inlet and outlet of segment 1, measured during the dehydration, are shown in Figure 6a. As can be seen, the temperature front proceeds through the bed from the top (level 4) to the bottom (level 1). Because there is no material in level 4, the temperature follows the exact same trend as the inlet temperature, and no endothermic reaction is observed. In other levels, steps can be seen in the temperature curves, which are caused by the energy used to dehydrate zeolite and release water.

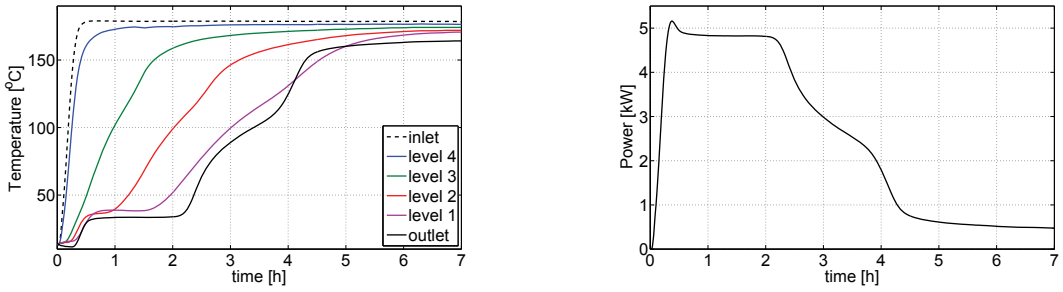

(a) Temperature at the inlet, outlet and center

(b) Thermal power transferred to the reactor.

Fig. 6: Results of the dehydration experiment in segment 1.

The thermal power transferred to the reactor is calculated based on $\dot{Q} = \dot{m}C_p(T_{out} - Tin)$ and is shown in Figure 6b. The average thermal power during 7 hours is around $2.47kW$, and the total energy is $17.29kWh$. As can be seen, most of the reaction is finished after 5 hours. The average power and total energy transferred to the reactor during the first 5 hours are $3.25kW$ and $16.24kWh$, respectively. Therefore, it is more efficient to stop the reaction after 5 hours.

The reactor is cooled down to the ambient temperature in the lab after the dehydration experiment, while the energy remains stored in the material. During the subsequent rehydration experiment in the pilot setup, air is directed to the humidifier to provide humid air. The humid air flows through the bed in order to rehydrate the material bed, release the stored energy and extract it in the form of thermal energy. The temperatures measured inside the bed and at the inlet and outlet of segment 1 during hydration are shown in Figure 7. As can be seen, the inlet temperature drops to around 10^oC because of the evaporation in the bubble column. The inlet humid cold air reacts with the charged material and releases heat. This can be seen in the form of a temperature rise in the bed. The reaction front passes through the bed as time passes. When the reaction is complete the temperature drops to the temperature of the cold inlet air.

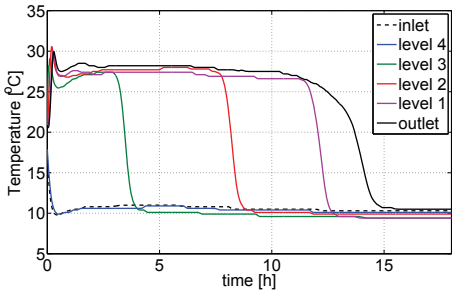

Fig. 7: Temperature at the inlet, outlet and center of the reactor segment 1 during the hydration experiment.

The same rehydration experiment is performed in the other segments in parallel with segment 1. The inlet and out temperature of the four segments are measured and shown in Figure 8a. The inlet temperature is the average of the measured temperatures at all inlets of the segments, which are almost equal and are around 10^oC. During hydration, humid air produced in the humidifier goes through the heater before entering the reactor. The system is designed in this way to provide the possibility of performing hydration experiments at an elevated inflow temperature. However, such experiments are not done in this work. In the present hydration experiment, the temperature increase in the segments is around 18^oC. This temperature increase is lower than what is expected (around 20^oC), which is probably because of a lower humidity generation in the bubble columns.

The humidity is also measured at the inlet and outlet of the four segments. The results are shown in Figure 8b. The measured humidity at the outlet of each segment is almost zero during the first 10 hours, since the entire water content in the inflow humid air is adsorbed by the material bed. After 10 hours, the humidity rises gradually to the same humidity as the inlet. The average inlet humidity is around $5.2g$ of water per kg of air. However, a higher humidity of around $7g/kg$ is expected at the inlet. This could be caused by a higher absolute pressure inside the humidifiers, which leads to a lower water content in the provided humid air.

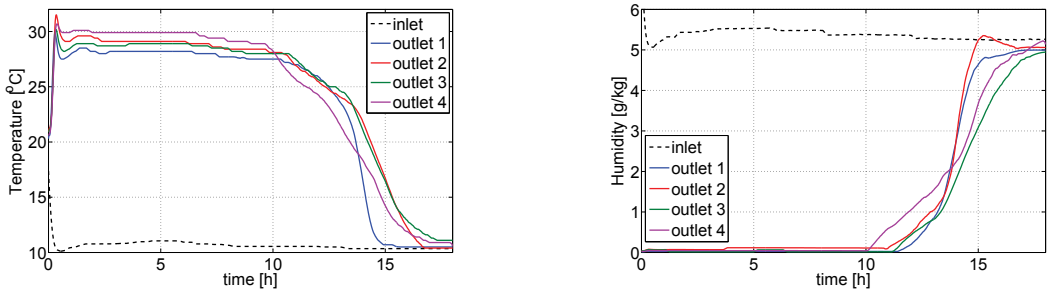

(a) temperature (b) humidity

Fig. 8: Temperature and humidity at the inlet and outlet of the four reactor segments during the hydration experiment.

Pressure is measured at the inlet and outlet of the four segments, and results are shown in Figure 9a. The pressure is also measured at the exhaust of the segments, and almost equals atmospheric pressure. Note that the pressure drop stays almost constant during the experiment, which means that swelling of the zeolite particles does not occur. The measured pressures slightly drop at the end of the experiment which can be related to the temperature drop at the end of the run. The average pressure drop over the bed in each segment is around $30Pa$. However, the biggest pressure

drop in the system is over the heater. The pressure before the heater is measured and it is around $0.2bar$ at an air flow rate of $50g/s$. This large pressure can explain the lower humidity provided by the bubble column as observed. In addition, the weakest point of the pilot, which prevents us from boosting the flow rate and subsequently the power, is the bubble column. The bubble column is the component which needs to handle the highest pressure, but seems not safe for that. For future research, it is important to fortify the bubble columns.

The released power from the segments during the rehydration experiment is calculated based on $P = \dot{m}C_p(T_{out} - Tin)$. The results are shown in Figure 9b. As can be seen, A high constant power of around $0.9kW$ is generated by each segment during the first 10 hours of the experiment. After that, the powers drop gradually, and they reach zero at around 17.5 hour. The power for segment 1 drops sharply and is back to zero after around 15 hours, which is the fastest among all the segments. The reproducibility of these results still needs to be investigated. The total maximum power generated by the pilot is around $3.6kW$, which lasts for almost 10 hours.

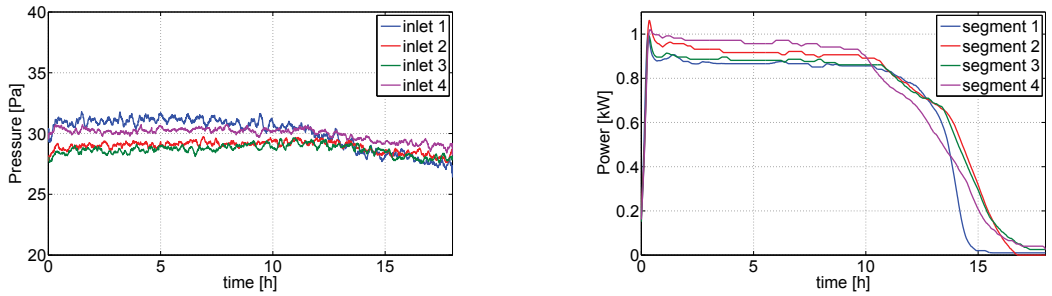

(a) Pressure at the inlet of the four segments

(b) Thermal power released from the four segments

Fig. 9: pressure drop and thermal power released during the hydration experiment.

The released energy and average power of each segment are calculated from the results presented in Figure 9b. These terms are calculated for two time intervals: from the start till 18 hours (the end) and from the start till 10 hours. The results are presented in Table 3. Almost 70 to 75 % of the total energy is released during the first 10 hours with high constant power (around $0.9kW$). In a real system, each segment should run for 10 hours individually to provide a constant power, and the energy associated with the last 5 to 8 hours can be recovered to the subsequent segment by running them in series. In addition, by considering the total energy supplied to segment 1 during the dehydration experiment (about $17.29kWh$ as discussed previously in this section), a total efficiency (energy released during rehydration divided by energy supplied during dehydration) of around 67% can be calculated.

Table 3: Energy content and energy density of the segments.

parameter	unit	1	2	3	4	average
released energy until 18 h	$[kWh]$	11.69	12.86	12.44	12.74	12.43
average power until 18 h	$[kW]$	0.65	0.71	0.69	0.71	0.69
released energy until 10 h	$[kWh]$	8.63	9.15	8.75	9.50	9.01
average power until 10 h	$[kW]$	0.86	0.91	0.87	0.95	0.90
Energy density of material	$[kWh/m^3]$	187	206	199	203	198
Energy density of reactor	$[kWh/m^3]$	102	112	108	111	108

Based on the total released energy and the volume of the material bed and the reactor segment, the energy densities on basis of the material and the reactor are calculated. An average energy density of $198kWh/m^3$ and $108kWh/m^3$

are calculated for material and reactor, respectively. The energy density of the reactor can be improved to almost $145kWh/m^3$, by filling more material in the top layer of the reactor. This means that the empty space at the top of the reactor, which is placed as the header distributor, will shrink, but this probably would not lead to less uniform flow through the bed. A much higher reactor energy density (close to the material energy density) will be ultimately achieved by removing the both empty spaces at the top and bottom of the reactor, in case the formation of non-reactive zones in the reactor can be avoided.

5. Conclusion

A large scale high power pilot is realized, consisting of four segments. The volume of each reactor segment (including empty header spaces) is $114.75L$, and each segment contains $62.5L$ of material. The total amount of zeolite 13XBF material in the segments is about $170kg$ ($250L$). Experiments are performed on the pilot in order to determine the energy storage density and to measure the power. For the charging process an inlet temperature of around 190^oC is used, and for the discharging process a water vapor pressure of around $1kPa$ ($5g$ of water per kg of air) at a temperature of about 10^oC is used. Average energy densities of $198kWh/m^3$ and $108kWh/m^3$ are calculated for material and reactor, respectively.

Each segment can be charged with about $17kWh$ (including losses) during 7 hours. Reducing the charging period to 5 hours, each segment is charged with $16kWh$, approximately, which is reasonably close to its maximum charging capacity. The total energy released during the discharge process is about $12kWh$, which is almost 70% of the supplied energy during 7 hours of charging process.

A maximum power of $0.9kW$ is achieved by each segment, which leads to a combined power of about $3.6kW$ lasting for almost 10 hours. This power can be improved by reducing the pressure drop over the system, and hence, increasing the humidity generated in the humidifier. During the first 10 hours of the discharge process, 70 to 75% of the total energy is released with a constant high power, and the rest is released during the final 5 to 8 hours of the discharge process where the power is gradually declining.

The pressure drop over the bed is only $30Pa$. Since the pressure drop over the bed is found to be small, the pressure drops in piping and over heat exchangers seems to be critical, in a real system. The largest pressure drop in the pilot setup is over the heater, which would not be part of a real thermochemical heat storage system.

Acknowledgement

This research has been made possible by the Smart Energy Regions Brabant (SERB) program, funded by the Province of North-Brabant.

References

[1] Saheb, Y.. Modernising building energy codes to secure our global energy future. The IEA Policy Pathway series; 2011.

[2] Rindt, C., Lan, S., Gaeini, M., Zhang, H., Nedea, S., Smeulders, D.M.. Phase change materials and thermochemical materials for large-scale energy storage. In: Continuous Media with Microstructure 2. Springer; 2016, p. 187–197.

[3] Zondag, H., Kalbasenka, A., van Essen, M., Bleijendaal, L., Schuitema, R., van Helden, W., et al. First studies in reactor concepts for thermochemical storage. In: Proc. Eurosun. 2008,.

[4] Bales, C., Gantenbein, P., Jaenig, D., Kerskes, H., Summer, K., van Essen, M., et al. Laboratory tests of chemical reactions and prototype sorption storage units. A Report of IEA Solar Heating and Cooling programme-Task 2008;32.

[5] Johannes, K., Kuznik, F., Hubert, J.L., Durier, F., Obrecht, C.. Design and characterisation of a high powered energy dense zeolite thermal energy storage system for buildings. Applied Energy 2015;159:80 – 86. URL: http://www.sciencedirect.com/science/article/pii/S0306261915010454. doi:http://dx.doi.org/10.1016/j.apenergy.2015.08.109.

[6] de Boer, R., Smeding, S., Zondag, H., Krol, G.. Development of a prototype system for seasonal solar heat storage using an open sorption process. In: Eurotherm Seminar# 99, Advances in Thermal Energy Storage. 2014, p. 28–30.

[7] Schnieders, J., Feist, W., Rongen, L.. Passive houses for different climate zones. Energy and Buildings 2015;105:71–87.

[8] Gaeini, M., Zondag, H., Rindt, C.. Effect of kinetics on the thermal performance of a sorption heat storage reactor. Applied Thermal Engineering 2016;102:520 – 531. URL: http://www.sciencedirect.com/science/article/pii/S1359431116303489. doi:http://dx.doi.org/10.1016/j.applthermaleng.2016.03.055.

[9] Gaeini, M., Zondag, H., Rindt, C.. 2017. International Journal of Heat and Mass Transfer submitted in 2016;.